Scientific Journal of Impact Factor (SJIF): 5.71

e-ISSN (O): 2348-4470
p-ISSN (P): 2348-6406

International Journal of Advance Engineering and Research Development

Volume 5, Issue 03, March -2018

STORAGE USE IN GRID-CONNECTED PV SYSTEM WITH MICROINVERTERS FOR REDUCTION OF INTERMITTENCE

Graosque, A. A. B.[1], Dias, J. B.[1], Dai-Prá, L. B.[2], Pillot, B. D. F.[1]

[1]*Laboratory of Photovoltaic Solar Energy, Graduate Program in Mechanical Engineering, University of Vale do Rio dos Sinos (UNISINOS)*
[2]*Laboratory of Environmental Sanitation, Graduate Program in Civil Engineering, University of Vale do Rio dos Sinos (UNISINOS)*

Abstract — *Grid-connected photovoltaic (PV) systems, in their classical configuration, do not have battery bank for energy storage, but how these systems are dependent on climatic conditions, which makes them an intermittent source, the application of energy storage is an alternative to reduce the variation of power produced and to improve the quality of energy delivered to the grid. This work proposed the installation of a grid-connected PV system with microinverters. The system was composed of two arrays, one in the classical configuration and the other one using energy storage. In addition to the installation of the PV system, a data acquisition was developed to improve the managing of the system. Each array was composed of one 265 W module and one 240 W microinverter of model SUNNY BOY-240. One of the arrays had a battery storage operating in the voltage of 24 V, with a nominal capacity of 200 Ah and a MPPT charge controller. The data acquisition and control unit has been configured for 1 and 10 s measurements. Through analyses, it was observed that energy storage in the grid- connected photovoltaic systems is very effective, mainly to reduce the power fluctuation delivered to the grid by the microinverter.*

Keywords-*Grid-connected PV System, Intermittence, Energy Storage, Microinverters, Photovoltaic Energy*

I. INTRODUCTION

The photovoltaic (PV) system is one of the fastest growing renewable energy sources and is also the most sensitive to fluctuations because it is directly dependent on climatic conditions, mainly solar radiation. On clear or overcast days, the variation in the power generation, in short intervals of time, is much-reduced [1]. Although, in partially overcast days, variations of 60% can occur in intervals of seconds [2].

The high variation in output power causes difficulties in the energy generation, as well as to generate transients that directly affect energy quality, impacting the magnitude of voltage, frequency, current and voltage harmonics, flicker effect and power factor [3]. Energy storage is one of the artifacts that can be used to reduce the intermittence, characteristic of the renewable energy sources such as photovoltaic and wind power [4].

Energy storage technologies such as batteries, supercapacitors and fuel cells are used with the aim of reducing the intermittence [5]. This experiment was carried out with microinverters grid-connected power. These devices are most often known to operate in the range of 100 to 300 W. The connection of the microinverters is directly to the photovoltaic modules, which makes it possible to better cover the diversity of roofs, reducing the problem with shading and increasing the energy efficiency of the installation compared to inverter systems in the string configuration [6]. The efficiency of the microinverters is mostly above 90% [7]; [8].

II. METHODOLOGY

The present work presents characteristics of an experimental research, that evaluated the efficiency of a PV system by measurements carried out in the applied system. The research is not intended to be conclusive. It is hoped to share reflections about the results and data acquisition obtained with the use of energy storage in photovoltaic systems connected to the electric grid.

2.1. System Description

The experiment consisted of two arrays, named array_1 and array_2, with microinverters connected to the power grid. Array_1 was in the configuration with energy storage, where a battery energy storage was placed in the input of one of the microinverters. To control the loading and unloading of the storage, a load controller with a Maximum Power Point Tracker (MPPT), normally used in autonomous systems, was installed.

Array_2 was in the classic grid-connected configuration, where the PV module is connected directly to the microinverter. The Multigate interfaces with the microinverters and the power grid, as well as manage data acquisition by the SunnyExplore platform.

Circuit breakers were installed to ensure exchange operations or even for a possible individual connection of each arrangement. Fig. 1 shows the complete diagram of the installed PV system.

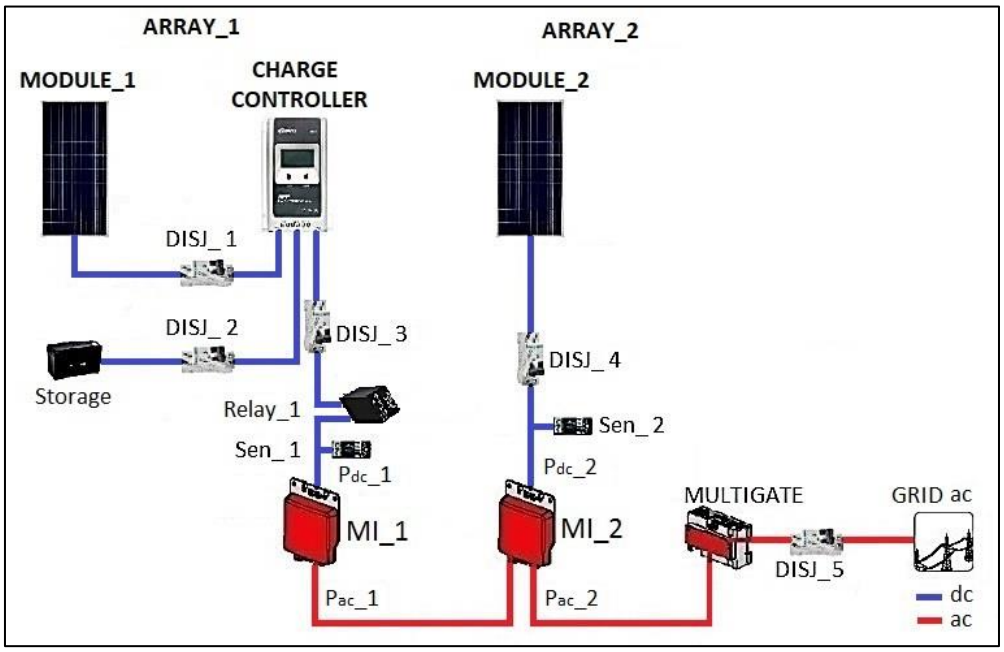

Fig. 1: Connection diagram of the photovoltaic system

The system was installed on the campus of the University of Vale do Rio dos Sinos (Unisinos), in Brazil. The photovoltaic modules were positioned in a horizontal angle of 20º and in an azimuth angle of 0º, in the geographic north direction. Control, protection and data acquisition devices were installed in a panel inside the Laboratory. The specifications of the main equipment used are described in Tab. 1.

Table 1. Specifications of the main equipment used

Equipment	Quantity	Characteristics
PV Module	2	SE-P265NPB-A4 - SUNEDISON
		Peak Maximum Power = 265 W_p
		Efficiency = 16.2%
Microinverter	2	SUNNY BOY 240-US – SMA
		Nominal Power = 240 W
Charge controller	1	TRACER 1210A – EPSOLAR
		Nominal Voltage 24 V
		On-Load Current = 10 A
		Battery Max Voltage = 32 V
Battery storage	1	Nominal Voltage = 24 V
		Current Capacity = 200 Ah
Data acquisition and control unit	1	Arduino AT Mega 2560
		Current Sensor – ACS712-20A

2.1.1. Equipment configuration. In the installation of photovoltaic equipment, the components must be configured in such a way that it is possible to extract the highest possible energy from the photovoltaic generator. The charge controller used in the array_1, with the MPPT mode as its working standard, requiring no parameter selection [9]. The MPPT has the function of optimizing the power extraction of the photovoltaic generator by means of continuous and periodic adjustment of the voltage and current values for each irradiance condition and module temperature, so that they are always working at a point of maximum power [10].

The microinverter of array_1 was configured to operate at a constant input voltage of 24 V, equivalent to the rated voltage of the storage. The microinverter of array_2 was setup in MPPT mode. Fig. 2 shows the installed photovoltaic modules and the panel with microinverters, charge controller and other equipment.

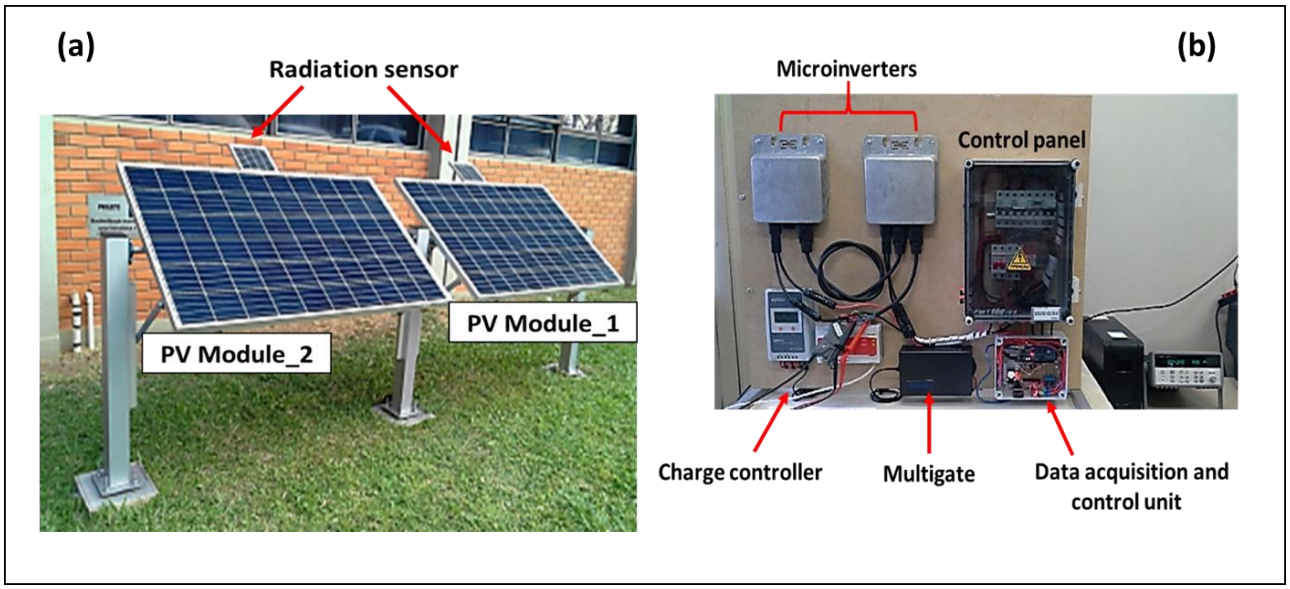

Fig.2: Installation of the system. (a) Installed photovoltaic modules; (b) Panel with microinverters, charge controller and other equipment's

2.1.2. Calibration of the data acquisition and control unit. After the development of the project and photovoltaic system installation, construction and calibration of the data acquisition and control unit was carried out and then the data collection was made.

The measurements of voltage and electrical current magnitudes were made at the input of each microinverter. The irradiance incident on each module was measured indirectly by the Agilent 34970A instrument, from photovoltaic modules of 5 W, calibrated and used as radiation sensors, installed in each main module.

For the measurement of the continuous electric current, the current sensor of Allegro model ACS712-20A was used. The sensor allows the measuring of electrical current up to 20 A. For each ampere of current passing through the sensor, a voltage of 100 mV is generated. This sensor has a response of 5 μs and a 5V supply [11]. The voltage values were measured from a voltage divider circuit (Fig. 3), where U_MI1 is the input voltage in the microinverter of the storage array_1 and U_MI2 is the input voltage of the classical array_2, A1 and A3 are indicators of connection in the Arduino platform.

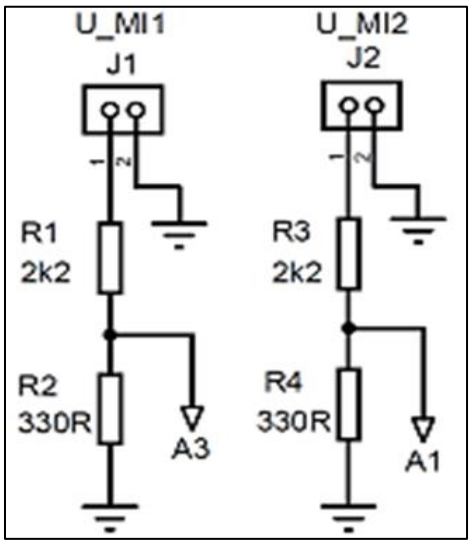

Fig.3: Voltage divider circuit

For data acquisition and control unit, the Arduino free development platform was used, where the variables were manipulated and stored on a memory card.

The calibration of the voltage and current values measured by the sensors was performed by comparing them with measurements synchronized with voltmeter and amperemeter ET-2550 (Fig. 4).

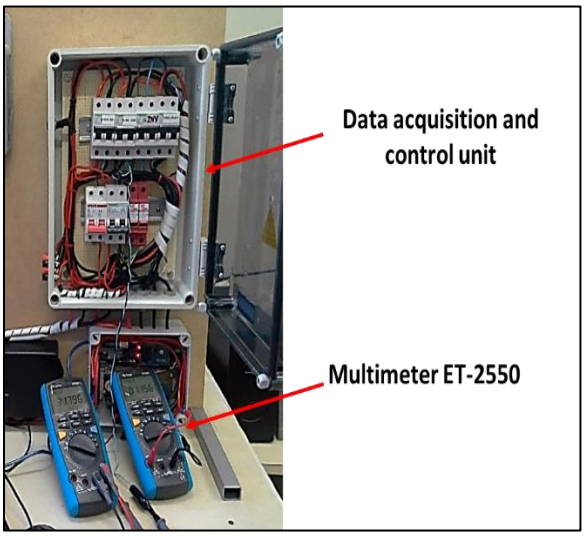

Fig. 4: Calibration of the data acquisition and control unit

Voltage and current measurements were performed with a one-second interval and the linear regression curve was generated, which represents the approximation of the values measured by the instrument and the respective values measured by the sensors.

In Fig. 5 (a), the U_S and U_I axes respectively indicate the voltage values measured in the voltage divider and read by the Arduino and the ET-2550 voltmeter. In Fig. 5 (b), the I_S and I_In axes respectively indicate the electric currents measured by the current sensor and the ET-2550 amperemeter. These measurements were performed at the entrance of the microinverter of the classical array.

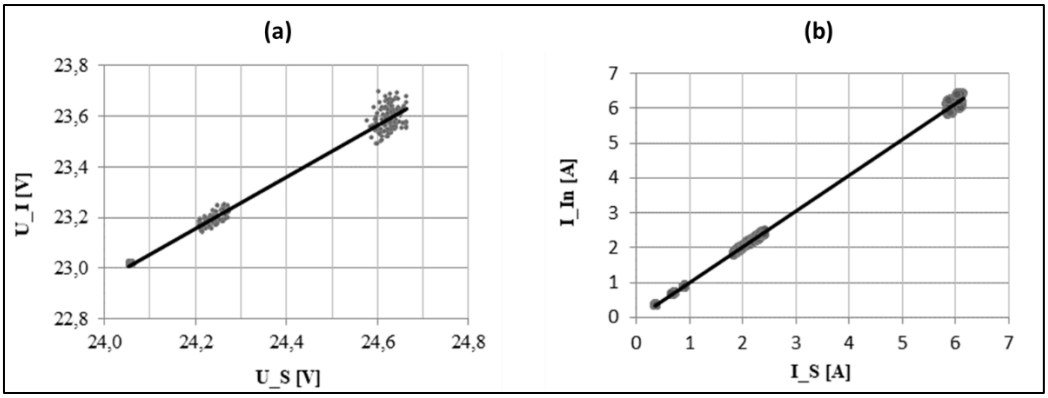

Fig. 5: Calibration curve of the measuring unit. (a) Voltage calibration curve; (b) Calibration curve of the electric current

From the calibration curve, the correct Equations for electric voltage in (1) and electric current in (2) were generated.

$$U_{dc-i} = 1.017U_{S-i} - 1.448 \quad (1)$$

$$I_{dc-i} = 1.029I_{S-i} - 0{,}053 \quad (2)$$

Where $U_{dc\text{-}i}$ is the corrected direct voltage value at the input of each microinverter and $U_{S\text{-}i}$ is the voltage read by the Arduino corresponding to each array. $I_{dc\text{-}i}$ is the corrected direct current at the input of each microinverter, $I_{S\text{-}i}$ is the value of the electric current measured by the current sensor to each array. These corrected values were used in the algorithm to determine the input power of each microinverter for each array, calculated by Eq. (3).

$$P_{dc-i} = I_{dc-i}U_{dc-i} \quad (3)$$

The power delivered to the grid $P_{ac\text{-}I}$ was calculated in Eq. (4), where $P_{dc\text{-}i}$ is the input power of each microinverter and η_{inv} is the average conversion efficiency in each microinverter, with the value of 0.91.

$$P_{ac-i} = \eta_{inv}P_{dc-i} \quad (4)$$

The efficiency was obtained from the relation between the AC at the output of the microinverter by the Fluke 43B instrument and the DC, by the microinverter input. In this step, some measurements were made for several loads. From the value obtained, an arithmetic average of 0.91 was calculated.

2.1.3. Analysis of uncertainties. Each measurement performed by the data acquisition and control unit has an uncertainty due to the sensitivity of the sensor and the measurement accuracy of the microcontroller. The measurement accuracy of the Arduino analog inputs is ± 0.3% and the accuracy of the ACS712-20A sensor is ± 1.5%. The combined uncertainty in DC measurement is calculated by Eq. (5), where ward is the uncertainty obtained with the Arduino measurement and wsen is the uncertainty obtained in the measurement with the current sensor. The calculated value was wi-I ± 1.5%, corresponding to a current of 9.0 ± 0.1 A.

$$W_{i-I} = \sqrt{{W_{ard}}^2 + {W_{sen}}^2} \quad (5)$$

The measurement of the continuous voltage is made by a voltage divider. The combined uncertainty was calculated by Eq. (6), where w_{volt} is the voltage divider measurement accuracy of ± 5%. The calculated result was $w_{i\text{-}V}$ ± 5%, corresponding to a voltage value of 35 ± 2 V.

$$W_{i-V} = \sqrt{{W_{ard}}^2 + {W_{volt}}^2} \quad (6)$$

For the combined uncertainty in the measurement of direct current power at the input of each microinverter, was considered the uncertainties of both the voltage and current, calculated in Eq. (7). The value found was ± 0.7%, corresponding to a power value of 258 ± 2 W. The efficiency uncertainty was ± 4%. The combined uncertainty of the power delivered to the grid *Wi-*$P_{a.c.}$ was ± 4%, corresponding to a power value of 228 ± 9 W.

$$W_{i-P_{dc}} = \sqrt{\left(\frac{\partial P_{dc-i}}{\partial U\_i} W_{i-U}\right)^2 + \left(\frac{\partial P_{dc-i}}{\partial I\_i} W_{i-I}\right)^2} \quad (7)$$

2.1.4. Energy quality in microinverters. The power quality is directly linked to the change in the waveform generated by the inverters in grid-connected power. Any alteration in frequency or amplitude, arising from interruptions, noises, disturbances or frequencies outside the fundamental, are perturbations known as harmonic distortions [12].

In Brazil, inverters and microinverters that are connected to the grid must comply with the ABNT NBR 16149:2013 standard, which establishes parameters for voltage, power, frequency, harmonics, waveform distortion and others. According to the cited norm, it is convenient for photovoltaic systems to deliver power with low levels of harmonic current distortion to the grid to ensure that no adverse effects occur on other equipment connected to the same grid. Tab. 2 shows the limits of current harmonic distortion established by [13].

Table 2. Current harmonic distortion limit

Harmonics	Limit
THD_i	< 5 %
Odd – 3^a to 9^a	< 4 %
Odd – 11^a to 15^a	< 2 %
Odd – 23^a to 33^a	< 1.5 %
Pairs – 2^a to 8^a	< 1.0 %
Pairs – 10^a to 32^a	< 0.5 %

The works of [14], [15], [16] and [17] shows that inverters or microinverters present harmonic distortion of THDi current above that allowed by NBR 16149, when working with an average load below 10%.

2.1.5. Array with battery storage. Storage mainly with batteries are very used in off-grid PV systems or together with hybrid inverters, whose purpose is to keep the load in operation when there is a lack of the electric grid [18].
In this study, the purpose of the storage was to reduce the fluctuation of the power supplied to the grid during the day and to store the energy generated by the PV modules on overcast sky days, where the load was low on the microinverter. During the night, the microinverter does not operated on the grid, even if there was energy stored in the batteries. For this situation, a condition was created, controlled from the power value of the classical array module. The condition established that the storage array was on the grid when the microinverter of the classical array had loads greater than 10%, equivalent to a power of 24 W. This condition is presented in Fig. 6, where an algorithm was performed in Arduino platform from this flowchart.

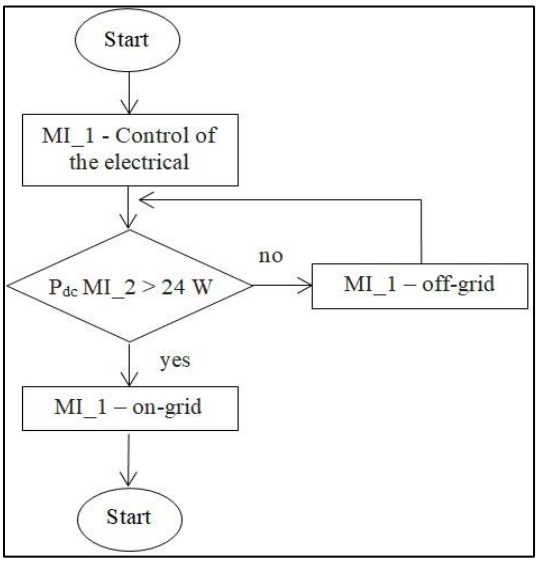

Fig. 6: Flow diagram for the storage array activation.

This condition was used because instead of providing the power grid with a high content of harmonics, above the values established by norm, the energy was stored, preventing such array to connect to the grid on overcast days. The algorithm used also allows to check whether the value will remain higher or lower than the 24 W, or if it is just an over-valued random pulse.

2.1.6. Period of data acquisition. The system came in operation on April 2017, where data collection started. The first values collected were for calibration of the data acquisition and control unit, as well as for efficiency determination. In the months of June and July, the data for intermittent analysis were collected, where partially overcast days were selected. To disregard the shading from trees, poles, light fixtures present near the PV modules, the daily time interval observed was from 11 to 15 h. This interval was also used in [19], due to variations at dawn and dusk. The periods of fluctuation analysis were 1 and 10 s. It should be noted that: the lower the time interval between the measurements, and the larger the database, maximum amplitude in the power variation is shorter by 1 s, when compared to a time interval of 10 s [20].

III. RESULTS

3.1. Condition on overcast sky day

For the overcast days, the intermittence was almost disregarded, since the energy production of the generator was maintained with low values, but in a constant way. In this situation, the energy generated by the PV module was not available to the grid, but stored in the battery storage, Fig. 7.

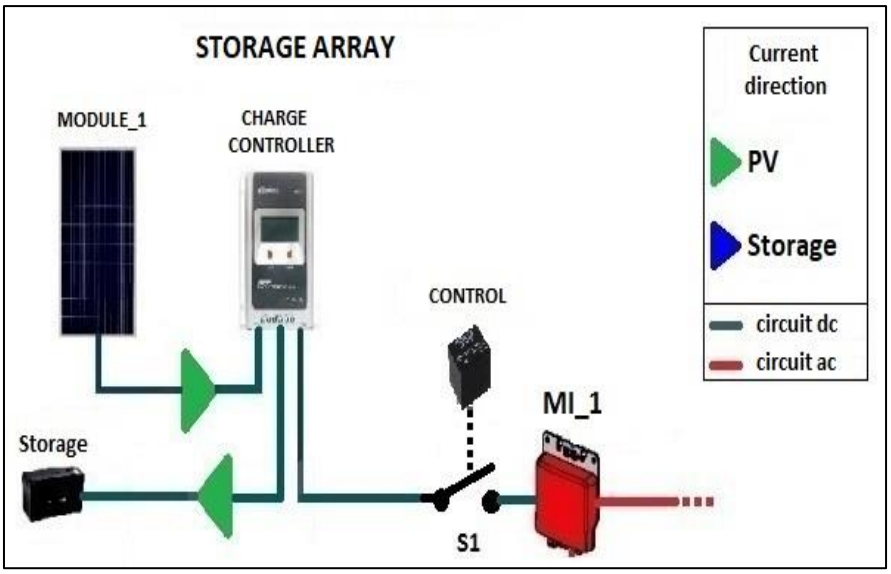

Fig. 7: Direction of the electric current in overcast sky days

Fig. 8 shows that, on an overcast day, the energy available for the power grid in the classic array was below 10 W throughout the day.

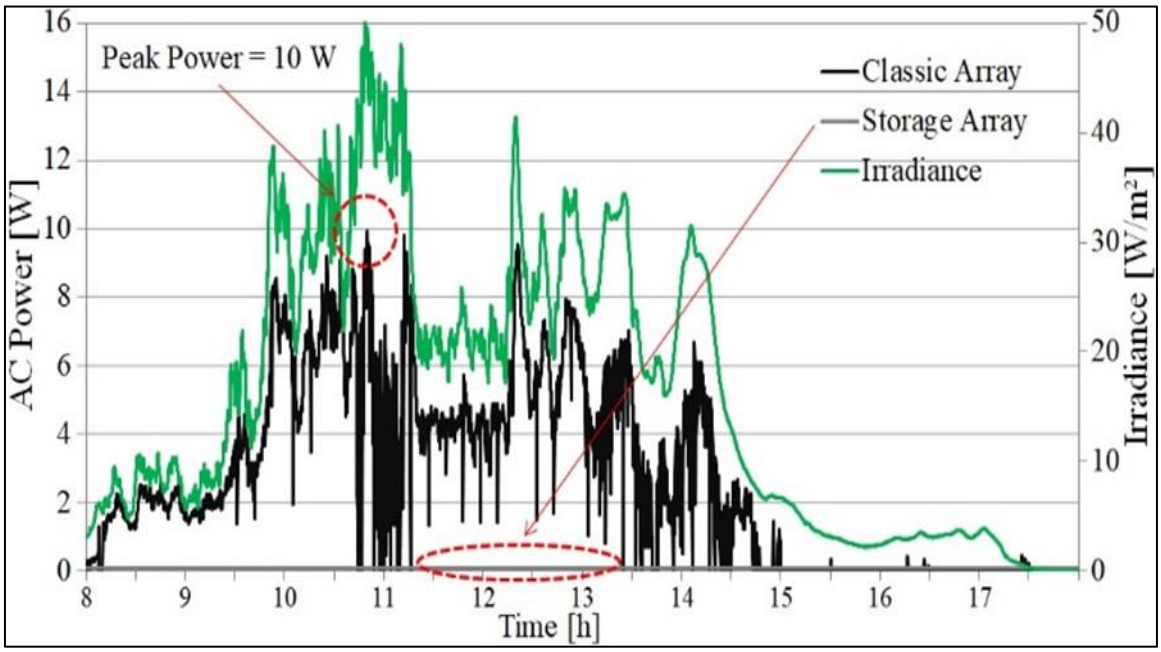

Fig. 8: System response on an overcast sky day

In that situation, the generated energy had a great number of harmonics, due to the low load of the microinverter. The S1 switch remains open, not allowing the microinverter to be connected to the grid. The energy produced by the PV module was stored in the batteries.

On another overcast day, it can be seen in Fig. 9 the result of the control system used. The control allows the storage array to supply power to the grid only when the classical array reaches power above 24 W and when the power is below that value, the storage array was off-grid and the energy generated by the photovoltaic module was stored in the batteries.

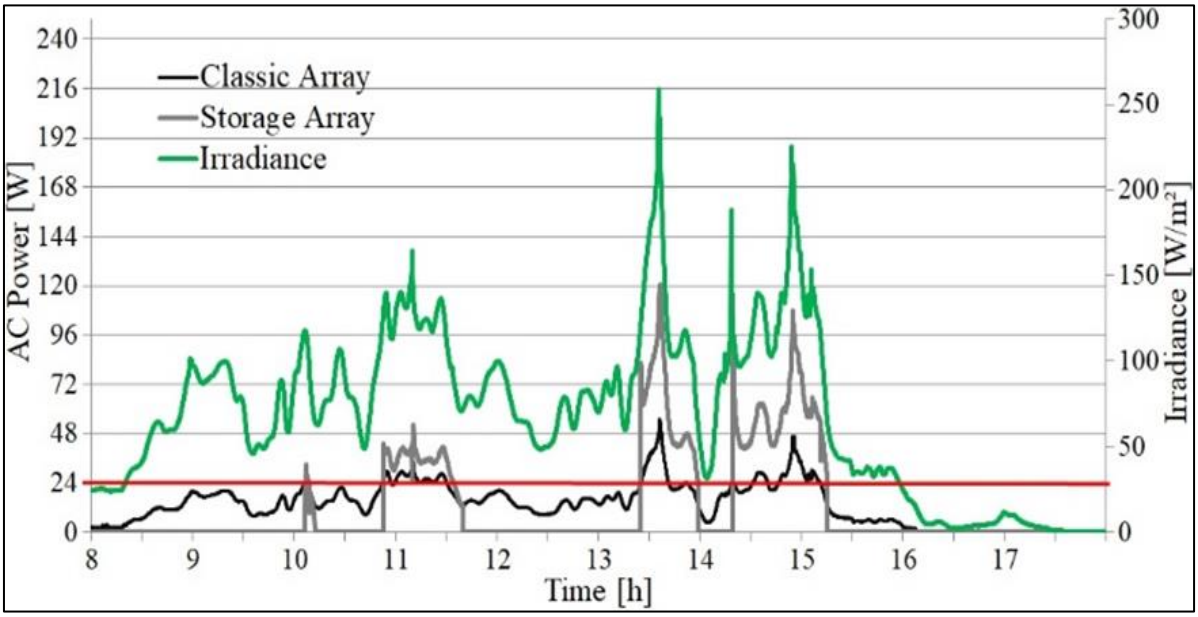

Fig. 9: System response on an overcast sky day

3.2 Clear sky day condition

In the clear sky days, there are no significant variations, in short intervals, of the irradiance incident on the PV modules. In that situation, the power that the storage array makes available to the power grid was close to the nominal power of the microinverter. The electric current generated by the module was drained by the microinverter and the rest was stored in the battery storage and that control was performed by the charge controller, Fig.10.

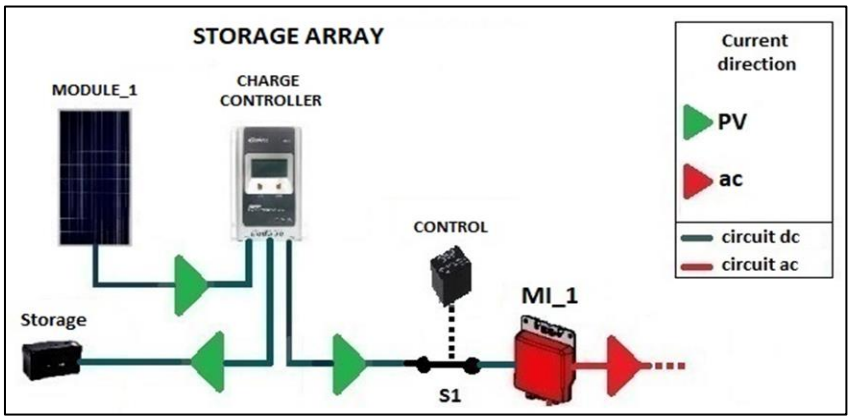

Fig. 10: Direction of the electric current in clear sky days

Fig. 11 shows, on a clear sky day, that the system did not showed a considerable fluctuation in power delivered to the power grid in the interval of 11 to 15 h. The abrupt power, dropped at 3:30 pm, occurred due to the shading of a pole near the PV module location. For analysis of the intermittence, that drop was disregarded. It is observed in this figure that the storage array delivers a constant power between 10 and 16 h, while the classical array delivers a power depending on the incident irradiance.

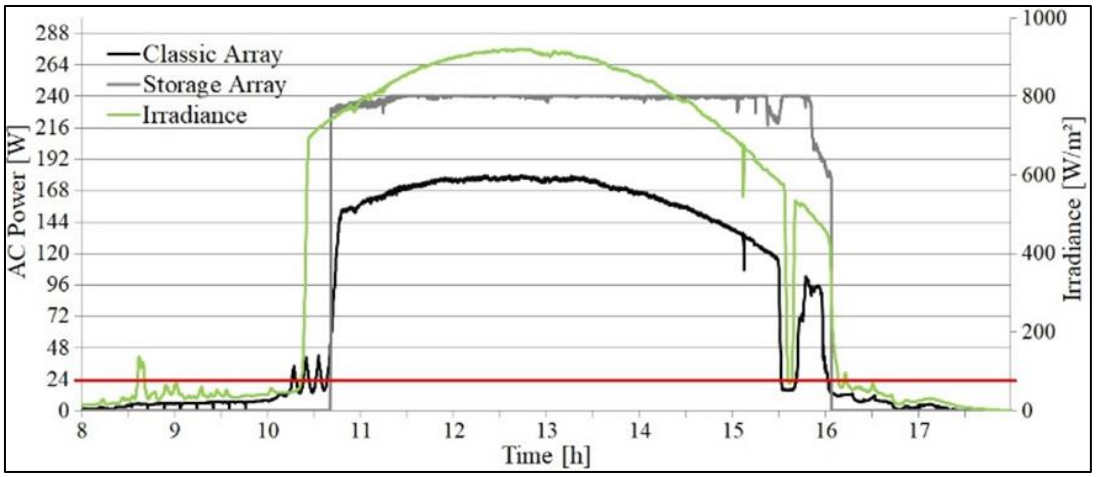

Fig. 11: Behavior of the system on a clear sky day

3.3 Partially overcast sky day conditions

In that condition, the direction of the electric current in the storage array, Fig. 12, was alternated in the microinverter between the PV module current, when the irradiance was high, and the storage when the irradiance was low.

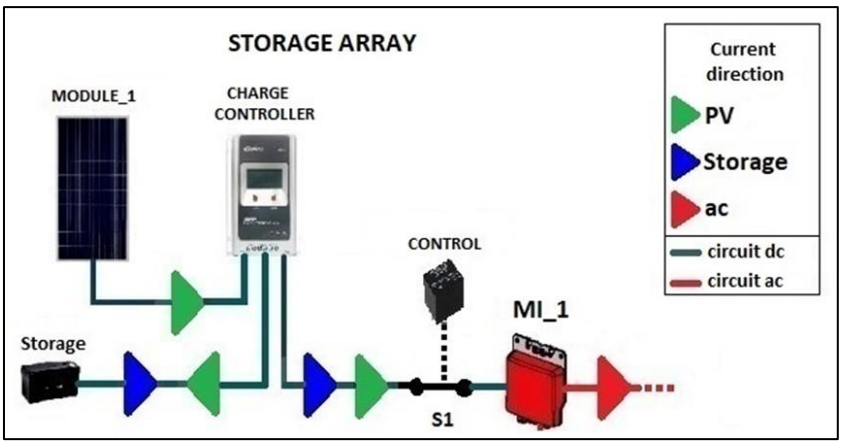

Fig. 12: Direction of the electric current in partially overcast sky days

The analysis of the system was performed in the interval of 11 to 15 h, period that the modules did not suffer shading of external structures, but variations of irradiance caused by the passage of clouds. Fig. 13 illustrates a classic day of partially overcast sky.

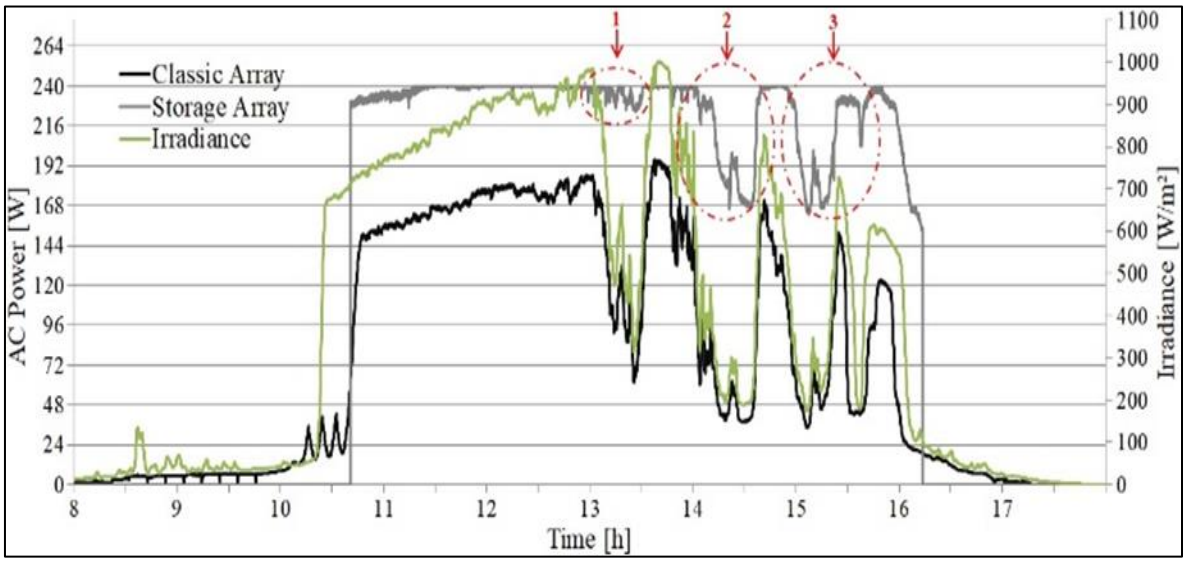

Fig. 13: Behavior of the system on a partially overcast sky day

In detail, point 1 shows the array with storage keeping the output power of the microinverter almost constant. Points 2 and 3 show the power generated with small variations. This variation of power is due to the battery storage not being in full load conditions.

With reference to work [19] and [20], the analysis is shown in number of power variation occurring during the determined time interval.

The analysis was performed in two periods, one with a measurement every 1 s and another every 10 s. The power variation was calculated by equation (8).

$$\Delta P = P(t + \Delta t) - P(t) \quad (8)$$

The power varied in values of rise, adopted as positive, and values of fall adopted negative. To better present the graphs and tables, fluctuation values lower than 1.5 W were disregarded. The first result is observed in Fig. 14, where the analysis period was 1 s.

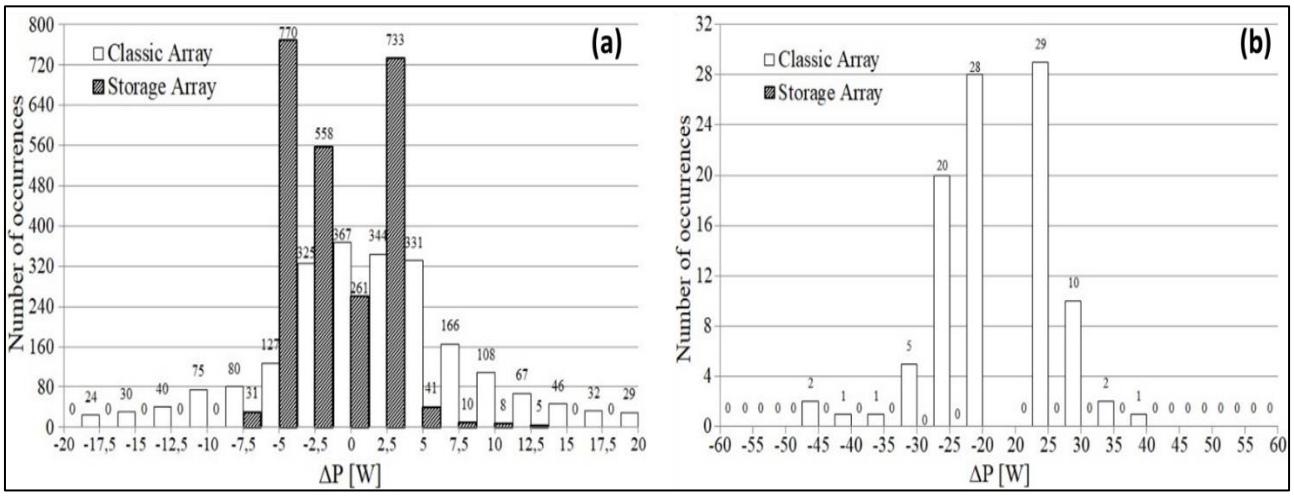

Fig. 14: Number of power variations AC. delivered to the grid with period of 1,0 s: (a) variation of power from 0 to 20 W; (b) variation that occurred from 20 W up to 60 W

The number above each bar represents the number of fluctuations that occurred in a specific power range. The painted bar shows the power variations that occurred in the storage array and the blank bar in the classic array. Fig. 14 (a) shows the fluctuation with a division at every 2.5 W between 0 and 20 W. The classical array showed fluctuations of 30 W, which represents a variation of more than 10% of the installed PV system. However, the storage array completely reduced fluctuations greater than 15 W of power in the analysis in 1s, evidencing its effectiveness for high variations. When analyzing the negative variations, the storage array was even more effective, eliminating the power reductions of 7.5 W.

The time to verify the behavior of the assembled system occurred mostly with a data collection interval of 10 s. The analysis with time interval of 10 s is illustrated in Fig. 15, that shows that there were possible high variations in power even in the storage array, due to the reduction of the load on the battery storage.

It can be observed that there are several positive and negative variations in symmetry. The point of greatest relevance is in Fig. 15 (c), which shows a reduction in the power delivered to the grid by the classic array of 124 W.

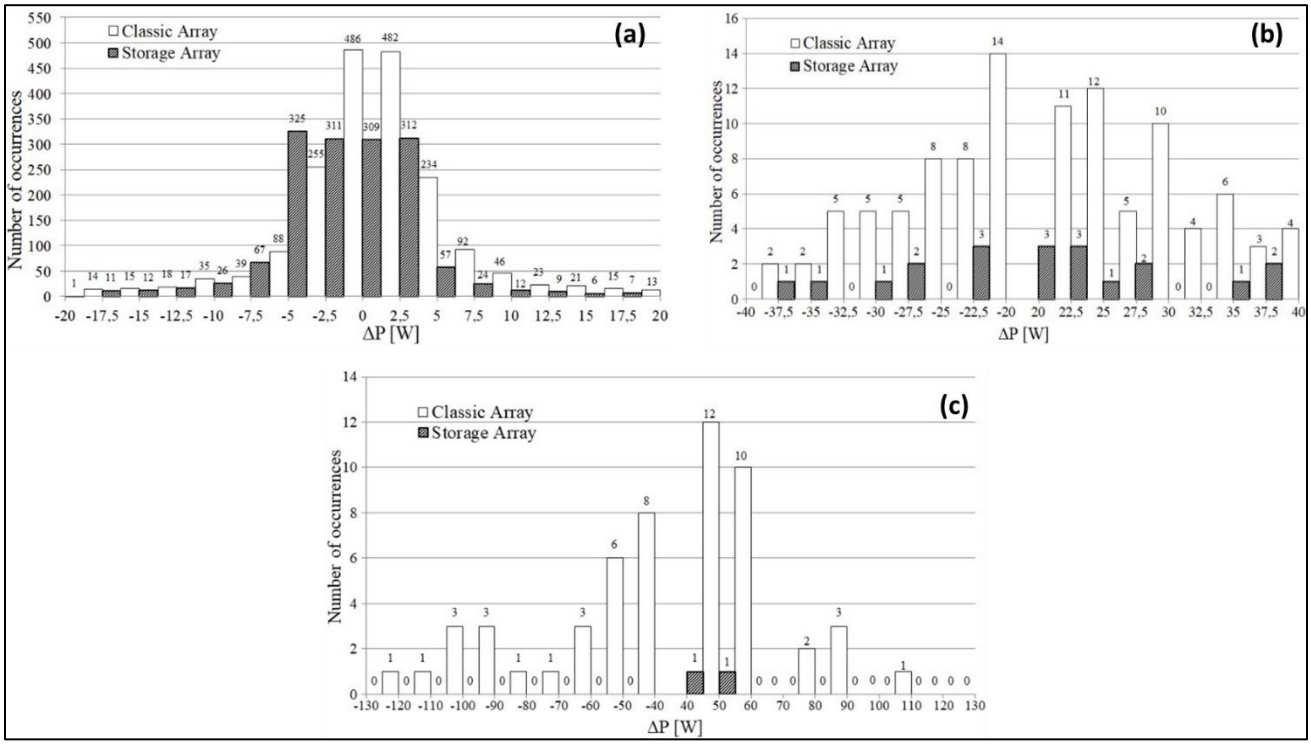

Fig. 15: Number of power variations AC delivered to the grid with a period of 10 s: (a) power variation from 0 to 20 W; (b) variation that occurred from 20 to 40 W; (c) power variation that occurred from 40 to 130 W

This value represents a variation of almost 60% of the value of the photovoltaic generator. In this situation, the storage array maintained the output power without intermittence.

Tab. 3 illustrates in a simplified way, for values in the range of 10 W, two sample periods, according to work of [20].
It is noted that, for the analysis interval of 10 s, more fluctuations occurred than in 1 s. The storage array presented a good result with a time interval of 1 s, eliminating the positive variations above 20 W and eliminating the negative variations above 10 W, that is, the output power remained constant.

Table 3. Number of power variations delivered to the grid with periods of 1 and 10 s: (a) positive power variation; (b) negative power variation

(a)		ΔP [+]												
		0-10 [W]	10-20 [W]	20-30 [W]	30-40 [W]	40-50 [W]	50-60 [W]	60-70 [W]	70-80 [W]	80-90 [W]	90-100 [W]	100-110 [W]	110-120 [W]	120-130 [W]
CLASSIC ARRAY	1 s	949	174	39	3	0	0	0	0	0	0	0	0	0
	10 s	854	72	38	17	12	10	0	2	3	0	1	0	0
STORAGE ARRAY	1 s	1263	13	0	0	0	0	0	0	0	0	0	0	0
	10 s	702	34	9	3	1	1	0	0	0	0	0	0	0

(b)		ΔP [-]												
		0-10 [W]	10-20 [W]	20-30 [W]	30-40 [W]	40-50 [W]	50-60 [W]	60-70 [W]	70-80 [W]	80-90 [W]	90-100 [W]	100-110 [W]	110-120 [W]	120-130 [W]
CLASSIC ARRAY	1 s	899	169	48	6	3	0	0	0	0	0	0	0	0
	10 s	868	82	35	14	8	6	3	1	1	3	3	1	1
STORAGE ARRAY	1 s	1359	0	0	0	0	0	0	0	0	0	0	0	0
	10 s	729	41	6	2	0	0	0	0	0	0	0	0	0

Fig. 13 also shows the energy produced in alternating current Equation (9) by the two arrays.

$$E_P = \int_{t_1}^{t_2} P_{ac-i}(t)dt \quad (9)$$

The energy produced by the arrays on July 4th, 2017, from 8 am to 6 pm, was obtained in 10 s intervals, Tab. 4.

Table 4. Energy produced by arrays on a partially overcast sky day

Arrangement	Energy produced (kWh)
Classic array	0.73
Storage array	1.25

IV. CONCLUSIONS

This work presented an alternative for the reduction of the intermittence in grid-connected photovoltaic systems. A PV system was set up with two arrays containing microinverters, one with energy storage in the batteries and another in the classical configuration. These arrays were analyzed and compared.

The use of battery, as a storage, performed satisfactorily. The storage array generally reduced power variations with values greater than 30 W, when analyzed in 10 s intervals, leaving the power delivery to the grid practically stable.

For the overcast sky days, the simple algorithm of control of drive of the array with storage was effective keeping the microinverter of the electric grid, which would be operating in low load and producing harmonic distortions for the grid. Already the energy generated by this photovoltaic array served to charger the battery.

It was also verified the number of variations and amplitudes of the electric power delivered to the grid by each microinverter in intervals of 1 and 10 s. The analysis with interval of 10 s showed to have a greater amplitude of the power generated by the classical array. The developed control system allowed in a simple way that the storage array was connected to the grid only for loads above 10%, storing the energy produced by the photovoltaic generator in low load of the microinverter.

As a complement to this study, it is suggested to carry out an economic feasibility analysis of the use of storage, a study of conversion losses as well as their design for grid-connected systems, since it has been shown that it is possible to deliver to the grid a power at certain time intervals. This can reduce the flashing and, also, the THDi content produced at the output of the inverters.

NOMENCLATURE

E_p	energy produced in alternating current (Wh)
I_{dc-i}	corrected direct current at the input of each microinverter (A)
I_{S-i}	electric current measured by the current sensor to each array (A)
P	Power (W)
P_{ac-i}	power delivered to the grid (W)
P_{dc-i}	is the input power of each microinverter (W)
t	time (s)
U_{dc-i}	corrected direct voltage value at the input of each microinverter (V)
U_MI1	input voltage in the microinverter of the storage array_1 (V)
U_MI2	input voltage of the classical array_2 (V)
U_{S-i}	voltage read by the Arduino corresponding to each array (V)
w_{ard}	uncertainty obtained with the Arduino measurement (V), (A)
w_{i-V}	voltage combined uncertainty (V)
w_{sen}	uncertainty obtained in the measurement with the current sensor (A)
w_{volt}	voltage divider measurement accuracy (V)

$W_{i\text{-}ac}$	combined uncertainty of the power delivered to the grid (W)
$W_{i\text{-}i}$	combined uncertainty in DC electric current DC measurement (A)
$w_{i\text{-}Pdc}$	combined uncertainty of the power DC (W)
ΔP	power variation (W)
Δt	time variation (s)
η_{inv}	average conversion efficiency in each microinverter (-)

ACKNOWLEGMENTS

Thanks to Unisinos (University of Vale do Rio dos Sinos) and CNPQ (National Council for Scientific and Technological Development) for financial support and Tecnosinos/SENAI Talent Scholarship Program, for providing the opportunity to accomplish this project.

REFERENCES

[1] Lew, D.; Miller, N.; Clark, K.; Jordan, G.; Gao, Z. (2010). Impact of high solar penetration in the interconnection. NREL Technical Report, NREL/TP-5500-49667.
[2] Mills, A.; Ahlstrom, M.; Brower, M.; Ellis, A.; George, R.; Hoff, T.; Kroposki, B.; Lenox, C.; Miller, N.; Stein, J.; Wan, Y. (2009). Understanding variability and uncertainty of photovoltaics for integration with the electric power system. Available: https://pubarchive.lbl.gov/islandora/object/ir%3A153901/datastream/PDF/view. Access: Dec., 14th 2016.
[3] Lopes, M. G. (2015). Análise dos impactos técnicos resultantes da variabilidade de curto prazo de sistemas fotovoltaicos. Dissertation (Master's in Electrical Engineering) - Pós-Graduação em Engenharia Elétrica e de Computação da Universidade Estadual de Campinas.
[4] Teleke, S.; Baran, M. E.; Bhattacharya, S.; Huang, A. Q. (2010). Rule-Based Control of Battery Energy Storage for Dispatching Intermittent Renewable Sources. In: IEEE Transactions on Sustainable Energy, vol. 1, no. 3, pp. 117–124.
[5] Shivashankar, S.; Mekhilef, S.; Morhlis, H.; Karimi, M. (2016). Mitigation methods of power fluctuation of photovoltaic (PV) sources – A review. In: ELSEVIER Renewable and Sustainable Energy Reviews, v.59, pp 1170-1184.
[6] Famoso, F.; Lanzafame, R.; Marnza, S. Scandura, P. F. (2015). Performance comparison between micro-inverter and string-inverter Photovoltaic Systems. In: ELSEVIER Energy Procedia, v. 81, pp. 526-539.
[7] Scholten, D. M.; Ertgrul, N.; Soong, W. L. (2013). Micro-Inverters in Small Scale PV Systems: A Review and Future Directions. In: IEEE Power Engineering Conference (AUPEC), Hobart, TAS, Australia, Sept 29th –Oct 3rd, 2013, pp. 1-6.
[8] Sher, H. A.; Addoweesj, K. E. (2012). Micro-inverters Promising solution in solar photovoltaics. In: ELSEVIER Energy for Sustainable Development, v. 16, pp. 65-72.
[9] EPSOLAR TECHNOLOGY CO. (2016). Manual de Instruções – Controlador Tracer-1210A. Available in: <http://www.epsolarpv.com/en/index.php/Product/pro_content/id/654/am_id/136> Access: Dec 14th. 2016.
[10] Pinho, J. T.; Galdino, M. A. (2014). Manual de Engenharia para Sistemas Fotovoltaicos. CEPEL – CRESESB Centro de Referência para Energia Solar e Eólica Sérgio de Salvo Brito. Rio de Janeiro, pp-244.
[11] ALLEGRO MICROSYSTEMS, LLC. (2017). Hall-effect-based current sensor IC. Available in:< http://www.allegromicro.com/en/Products/Current-Sensor-ICs/Zero-To-Fifty-Amp-Integrated-Conductor-Sensor-ICs/ACS712.aspx> Access: Jun 15th, 2017.
[12] Martinho, E. (2013). Distúrbios da energia elétrica. 3rd ed., v. 1, Érica Ed. São Paulo: 2013, pp.236 – 236.
[13] Associação Brasileira de Normas Técnicas - ABNT. 16149/2013, Características da interface de conexão com a rede elétrica de distribuição de sistemas fotovoltaicos. Rio de Janeiro, 2013. 12p. Available in: http://abntcatalogo.com.br/norma.aspx?ID=195959. Access: Dec. 14th 2016.
[14] Rampinelli, G. A.; Krezinger, A. (2011). Estudo da qualidade da energia elétrica injetada à rede por inversores utilizados em sistemas fotovoltaicos. In: ASADES, v. 15, pp. 65-72.
[15] Schenkel, G. (2015). Monitoramento e análise de um sistema fotovoltaico conectado à rede com uso de microinversor. Dissertação (Mestrado em Engenharia Mecânica) - Pós-Graduação em Engenharia Mecânica, UNISINOS, São Leopoldo.
[16] Chicco, G.; Schilabbach, J.; Spertino, F. (2005). Characterization and assessment of the harmonic emission of grid-connected photovoltaic systems. In: IEEE Russia Power Tech, pp.1-7.
[17] Ortega, M. J.; Hernández, J. C.; García, O. G. (2013). Measurement and assessment of power quality characteristics for photovoltaic systems: Harmonics, flicker, unbalance, and slow voltage variations. In: ELSEVIER Electric Power Systems Research, v. 96, pp. 23-35.

[18] Bellinaso, L. V.; Michels, L. (2016). Inversores Fotovoltaicos Híbridos com Armazenamento de Energia em Baterias – Classificação, Modos de Operação e Princípios de Funcionamento. In: VI Congresso Brasileiro de Energia Solar (CBENS), Belo Horizonte, Brasil, April 4th – 7th, 2016, pp. 1-6.

[19] Maskell, D. L.; Ramasubramanian, S.; Qing, X. (2015). Module-based Storage for Regulating PV Power Intermittence at the Point of Generation. In: IEEE Photovoltaic Specialist Conference, New Orleans, LA, USA, Jun 14th - 19th, 2015, pp.1-5.

[20] Sayeef, S.; Heslop, S.; Cornforth, D.; Moore, T.; Percy, S.; Ward, J. K.; Berry, A.; Rowe, D. (2012). CSIRO Solar Intermittence: Australia's Clean Energy Challenge. Characterizing the Effect of High Penetration Solar Intermittence on Australian Electricity Networks. [Online]. Available: https://publications.csiro.au/rpr/download?pid=csiro:EP121914&dsid=DS1. Access: Dec 14th 2016.

